



저작자표시-비영리-변경금지 2.0 대한민국

이용자는 아래의 조건을 따르는 경우에 한하여 자유롭게

- 이 저작물을 복제, 배포, 전송, 전시, 공연 및 방송할 수 있습니다.

다음과 같은 조건을 따라야 합니다:



저작자표시. 귀하는 원저작자를 표시하여야 합니다.



비영리. 귀하는 이 저작물을 영리 목적으로 이용할 수 없습니다.



변경금지. 귀하는 이 저작물을 개작, 변형 또는 가공할 수 없습니다.

- 귀하는, 이 저작물의 재이용이나 배포의 경우, 이 저작물에 적용된 이용허락조건을 명확하게 나타내어야 합니다.
- 저작권자로부터 별도의 허가를 받으면 이러한 조건들은 적용되지 않습니다.

저작권법에 따른 이용자의 권리는 위의 내용에 의하여 영향을 받지 않습니다.

이것은 [이용허락규약\(Legal Code\)](#)을 이해하기 쉽게 요약한 것입니다.

[Disclaimer](#)

Thesis for the Degree of Master of Engineering

Shore-to-Sea Maritime Visible Light Communication

by

Hyeong-Ji Kim

Department of Information and Communications Engineering

The Graduate School

Pukyong National University

February 2016

Shore-to-Sea Maritime Visible Light Communication

연안 대 해상 가시광통신

Advisor: Prof. Yeon-Ho Chung

by

Hyeong-Ji Kim

A thesis submitted in partial fulfilment of the requirements
for the degree of

Master of Engineering

in Department of Information and Communications Engineering,
The Graduate School, Pukyong National University

February, 2016

b

Shore-to-Sea Maritime Visible Light Communication

A dissertation

by

Hyeong-Ji Kim

Approved by :

Professor Shin-Il Jeong,
(Chairman)

Professor Jee-Youl Ryu,
(Member)

Professor Yeon-Ho Chung,
(Member)

February, 2016

Table of Contents

List of Figures	iii
List of Tables.....	v
Abstract	vi
1. Introduction	1
1.1. Visible Light Communication	1
1.2. Motivations and Research Objectives.....	2
1.3. Chapter Organization.....	3
2. Maritime Wireless Communication	5
2.1. Current Maritime Wireless Communication	5
2.2. Limitation of Conventional Maritime Communication	7
2.3. Maritime Visible Light Communication (MVLC)	8
3. Description of Maritime Environments	9
3.1. Sea Wave.....	9
3.2. Atmospheric Turbulence.....	14
3.2.1. Log-Normal Turbulence Model	14
3.2.2. Gamma-Gamma Turbulence Model.....	15
4. MVLC System Design.....	17
4.1. MVLC Channel Model	18
4.2. MVLC Receiver	20
5. Performance Analysis of the MVLC System	22
5.1. Shore-to-Sea Transmission in MVLC	22
5.1.1. Shore-to-Sea Visible Light Transmission.....	22
5.1.2. Performance Analysis	24

5.2.	Shore-to-Sea MVLC using Color Clustered MIMO	27
5.2.1.	Color Clustered MIMO VLC	27
5.2.2.	Performance Analysis	30
5.3.	Time-Code Diversity (TCD) Scheme for MVLC.....	31
5.3.1.	TCD Scheme for MVLC.....	32
5.3.2.	Performance Analysis	36
5.4.	MVLC Links Employing Multi-hop Relay.....	37
5.4.1.	Multi-hop Relay based MVLC.....	38
5.4.2.	Performance Analysis	42
5.5.	MVLC in Fog Conditions	45
5.5.1.	Analysis Fog Conditions for MVLC	45
5.5.2.	Performance Analysis	46
6.	Conclusions	49
	References	52
	List of Publications	59
	Journal Papers:	59
	Conference Papers:.....	60
	감사의 글.....	ix

List of Figures

Figure 2.1. Maritime communication for e-Navigation conception	6
Figure 3.1. Sea surface from the spectra under sea state 5: (a) PM, (b) JS... 13	
Figure 4.1. MVLC network.....	17
Figure 4.2. Maritime channel modeling.....	18
Figure 4.3. Receiving plane (10 m × 10 m)	20
Figure 4.4. BER performance comparison relative to PD physical area.	20
Figure 5.1. Shore-to-sea channel model: (a) Sea state 4, (b) Sea state 8.	24
Figure 5.2. Simulated proposed channel with PM spectrum: (a) SNR, (b) BER.	25
Figure 5.3. Simulated proposed channel with JS spectrum: (a) SNR, (b) BER.	26
Figure 5.4. BER performance of the MVLC system under different sea states.	26
Figure 5.5. Color-clustered MVLC system (a) Conceptual design, (b) RG LED array.....오류! 책갈피가 정의되어 있지 않습니다.	
Figure 5.6. Block diagram of the proposed system.	29

Figure 5.7. Performance analysis of MVLC link: (a) Conventional VLC, (b) Color Clustered MIMO based MVLC.....	31
Figure 5.8. Block diagram of the TCD scheme: (a) Transmitter, (b) Receiver.오류! 책갈피가 정의되어 있지 않습니다.	
Figure 5.9. BER performance comparison of OOK and TCD MVLC systems with the sea states and log-normal turbulence from JS model...	36
Figure 5.10. Multi-hop relay MVLC system.....	38
Figure 5.11. PD array-based VLC.	40
Figure 5.12. Comparison of BER performance over each gamma-gamma turbulence strength	42
Figure 5.13. BER performance relative to the received power level.....	43
Figure 5.14. BER performance relative to the number of hops with diversity combining techniques	44
Figure 5.15. Kim model for visibility for T_{th} of 2% and a range of RGB LED.	46
Figure 5.16. Shore-to sea transmission channel modeling: Sea state and fog condition.....	46

Figure 5.17. Comparative analysis of BER performance for MVLC link: (a)
Utilizing various color wavelengths in thin fog, (b) Under various
fog conditions using red color wavelength. 47



List of Tables

Table 2.1. IMO definition of sea area	5
Table 3.1. Sea state parameters	12
Table 3.2. Weak to strong turbulence regimes	16
Table 4.1. Simulation parameters of the MVLC system	19



Shore-to-Sea Maritime Visible Light Communication

Hyeong-Ji Kim

Department of Information and Communications Engineering, The Graduate School,
Pukyong National University

Abstract

A new wireless technology known as visible light communication (VLC) came into limelight with the advent of light emitting diodes (LEDs). VLC is a communication method using LEDs, where blinking of an LED is used for communication and illumination simultaneously. LED communication offers innovative wireless technologies in terms of communication speed, flexibility, usability and security. Unseen by the human eye, this variation is used to carry high-speed data, thereby creating wireless communication network using existing light resources in order to achieve low-cost communication. Currently the widespread use of LEDs in maritime applications presents a multitude of opportunities for visible light based maritime communications. Conventional maritime wireless communications rely predominantly on radio frequency (RF), which suffer from high cost with low transmission speed and scarce operation spectrum. To overcome these limitations in maritime communications, VLC can be considered an alternate technology in maritime environments. This thesis provides a detailed analysis of VLC under various atmospheric and sea conditions, which will eventually lead to significant improvement in communication range as well as link performance in maritime environments, thus leading to a low-cost, high-speed wireless link in the shore-to-sea maritime VLC (MVLC) system.

In the first study, for providing an efficient VLC link for maritime environments, it is important to analyze the effects of transmission under sea states (spectrum of sea waves due to blowing wind, atmospheric turbulence, etc.). Computer simulations are conducted based on the Pierson-Moskowitz (PM) and JONSWAP (JS) spectrum models with various sea states for analysis. The transmission system presented for shore-to-sea communication considers unique properties of maritime environments where wave height, wind speed, etc. exist.

Secondly, the thesis presents a MVLC scheme using color clustered multiple-input and multiple-output (MIMO) for satisfying International Association of Lighthouse Authorities (IALA) requirements for maritime buoyage system. Selection combining is performed at the receiver, producing diversity effect within that color cluster. The simulation results show the maritime link quality analyzed in terms of coverage distance and bit error rate (BER) performance provides an efficient MVLC and also offers sufficient illumination from high power LEDs.

The next study is a novel time-code diversity (TCD) scheme using the delayed versions of the original signal and orthogonal Walsh codes for MVLC system. The proposed TCD scheme has an advantage of simplicity to achieve a reasonable diversity gain resulting in a significant performance improvement, compared with related schemes such as adaptive optics and forward error correction for maritime environments.

In the later part of the thesis, a multi-hop decode-and-forward (DF) relay based VLC system is proposed to provide an efficient maritime link covering a longer distance with adequate performance in maritime environments. The performance of the proposed multi-

hop VLC system over maritime channels with DF relay is further improved using receiver diversity with combining techniques.

The quality of a VLC link in the troposphere is strongly influenced by weather conditions such as fog, rain and snow. Thus, the final study in the thesis work focuses on analyzing the link quality of MVLC system under foggy conditions. Investigation of communication link under fog condition is important for a MVLC system, as it causes severe loss of signals as compared to signal fading phenomenon. Computer simulations were conducted considering fog condition to analyze MVLC system in terms of BER and coverage distance.



1. Introduction

1.1. Visible Light Communication

Visible Light Communication (VLC) refers to optical wireless communication system that carries information by modulating light in the visible spectrum from 380 to 780 nm along with providing illumination [1, 2]. VLC transmits data by intensity modulating optical sources, such as light emitting diodes (LEDs) and laser diodes, flashing of the light actually happen much faster than human eyes can detect. Interest in VLC has grown rapidly with the growth of high power LEDs in the visible spectrum. The motivation to use the illumination light for communication is to save energy by exploiting the illumination to carry information and in comparison to radio frequency (RF) technology, while using the existing infrastructure of the lighting system. The necessity to develop an additional wireless communication technology is the result of the almost exponential growth in the demand for high-speed wireless connectivity.

The first works advancing this possibility were published by Pang and Nakagawa, reporting the usage of LEDs to communicate in both indoor and outdoor environments. Emerging applications that use VLC include: a) indoor communication where it augments WiFi and cellular wireless

communications [3]; b) communication wireless links for the internet of things (IOT) [4]; c) communication systems as part of intelligent transport systems (ITS) [5]; and d) wireless communication systems in hospitals [6].

1.2. Motivations and Research Objectives

In the study of this research, following aspects are considered for the maritime VLC (MVLC) systems.

- The conventional maritime wireless communications at sea rely mainly on satellite links that are expensive and relatively slower than high frequency (HF) and very high frequency (VHF). RF based maritime communication systems satisfy communication and navigation needs at the expense of high cost and low transmission speed. Moreover, it suffers from insufficient dedicated operation spectra. For this reason, maritime communications need an advanced technology to satisfy the demand of high speed transmission for sea users.
- To provide an efficient VLC link for maritime environments, it is important to analyze the effects of transmission under various

atmospheric conditions and sea states (spectrum of sea waves due to blowing wind, atmosphere turbulence, etc.).

- To use already available infrastructure like lighthouse as transmitter, beacons and buoys as receiver, for communication purpose.

With these motivations, the study in this thesis considers the following objectives.

- i. To consider the maritime condition for VLC.
- ii. To improve performance of MVLC using:
 - Color clustered Multiple-input and multiple-output (MIMO)
 - Time-Code Diversity (TCD)
 - Multi-hop relay
- iii. To improve throughput and link quality of VLC systems, for high-performance transmission in maritime environment.

1.3. Chapter Organization

The remaining chapters in this thesis are outlined as follows. Chapter 2 introduces conventional maritime wireless communication for MVLC. In Chapter 3 maritime environment is analyzed under sea state and atmospheric

turbulence for MVLC. Chapter 4 describes the VLC system designed for maritime environment. The MVLC system is analyzed for fundamental performances such as power reception and channel dispersion. The simulation based studies are presented in Chapter 5. Chapter 6 concludes the study considering all the experimental analysis.



2. Maritime Wireless Communication

2.1. Current Maritime Wireless Communication

Conventional maritime wireless communication operates in various RF bands, e.g. VHF operates with cellular mobile telecommunication systems (GSM, UMTS, etc.) and satellite communications systems (INMARSAT, VSAT, etc.). The radio types for sailing vessels are defined by International Maritime Organization (IMO) and International Telecommunication Union (ITU) [7]. Further, IMO defined the maritime wireless communication according to technology and communication coverage for Global Maritime Distress and Safety System (GMDSS), as in Table 2.1 [8].

Table 2.1. IMO definition of sea area

Sea Area	Technology	Communication Coverage
A1	VHF	Coast (20~30 miles)
A2	MF	Offshore (about 100 miles)
A3	INMARSAT/HF	70° N and 70° S
A4	HF, MF, VHF	The remaining sea areas

e-Navigation is a concept of maritime safety and security formulated and launched by IMO [9]. In particular, it will go into some depth on the need for shore to sea digital communication technology.

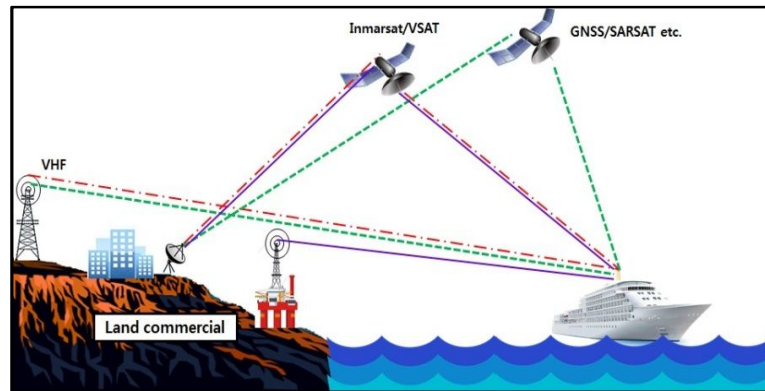


Figure 2.1. Maritime communication for e-Navigation conception

In Singapore, a project called TRI-media Telematic Oceanographic Network (TRITON) based on IEEE 802.16 implemented a mesh network for maritime communication using onshore stations, ships and buoys as communication nodes with the objective to develop a system for high-speed and low-cost maritime communications in narrow water channels and shipping lanes close to the shore [10].

European Space Agency (ESA) introduced Wired Ocean Project [11]. The intent of this project is to establish, on a commercial basis, cost-effective broadband IP-based communications services to ships. But the cost is still expensive and size of the terminal, especially stabilized Ku-band equipment, both receive-only and VSATs (Very Small Aperture Terminal).

2.2. Limitation of Conventional Maritime Communication

Maritime wireless communication is, however, differentiated from its terrestrial counterpart, because service environments are distinctly different. Global maritime communication between sea users and the rest of the world is technically developed and provided, but at a high cost. It is based on the electronically collected maritime data information on-board and ashore to enhance berth to berth navigation and related services at sea and also to protect the marine environment. Sea users need a high-speed and low-cost maritime wireless communication like on land. However, current wireless communications at sea mainly rely on satellite links that are relatively slow than HF and VHF or on expensive Inmarsat. Like on land, sea users also need a high-speed, low-cost maritime wireless communication and special service (Mobile Telemedicine in maritime [12], Container Tracking [13], etc.). Therefore, new technology is needed to improve existing maritime communications.

2.3. Maritime Visible Light Communication (MVLC)

In various areas of VLC in maritime environment, a few interesting reports have been documented. The underwater VLC was presented in [14]. In maritime environments, VLC can be applied to existing infrastructure such as lighthouses and maritime transceivers (marine beacons, buoys). Most of the lighthouses that use electric lamps are switched to LEDs nowadays, because life span, efficacy and power consumption of an LED are far better than conventional electric lamp. As part of a pioneering initiative, the Lighthouse Sub Project [15] started activity from September 2007 for the realization of the long-distance VLC using an existing LED lighthouse. The project was able to record a transmission rate of 1,200 bps at a distance of 1 km and a transmission rate of 1,022 bps at a distance of 2 km by using image sensor based VLC. However, this project was conducted in silent sea conditions and fails to perform a study on the feasibility of MVLC under various sea states. Thus, further investigations under various ocean and atmospheric conditions are necessary to establish a comprehensive MVLC system.

3. Description of Maritime Environments

Maritime communication environments have a unique property where sea surface movement is usually observed and subsequently periodic degradation exists. It is mainly characterized by this sea surface movement, together with radio propagation and Fresnel effect [16]. With the motivation for providing an efficient VLC link for maritime environments, it is important to analyze the effects of transmission under various atmospheric conditions and sea states (spectrum of sea waves due to blowing wind, atmosphere turbulence, etc.).

3.1. Sea Wave

Sea waves are generated by the effect of wind over the ocean surface. The sea spectra are used to provide an insight into the movement of sea surface in oceanography and ocean engineering. The waves are described only with a characteristic wave height (e.g., the significant wave height) and a characteristic period (e.g., the significant wave period or the peak period, i.e., the inverse of the peak frequency of the spectrum) or with a universal one- or two-dimensional spectrum [17]. The most accepted and renowned mathematical models for the analysis of sea spectra are one-dimensional

spectrum: the Pierson-Moskowitz (PM) spectrum and the JONSWAP (JS) spectrum.

The PM spectrum is given by [17]

$$E_{PM}(f) = a_{PM} g^2 (2\pi)^{-4} f^{-5} \exp\left[-\frac{5}{4}\left(\frac{f}{f_{peak}}\right)^{-4}\right] \quad (3.1)$$

where a_{PM} is energy scale, f is the wave frequency in Hz, g is the gravitational acceleration, and f_{peak} is the peak frequency. The peak frequency depends only on the wind speed. The PM spectrum is assumed that if the wind blew steadily for a long time over a large area, the sea waves would come into equilibrium with the wind.

On the other hand, the JS spectrum is based on non-linear and wave-wave interactions for very long times and distances by analyzing data collected during the Joint North Sea Wave Observation Project [18]. The JS spectrum is given by [17]

$$E_{JS}(f) = a_{JS} g^2 (2\pi)^{-4} f^{-5} \exp\left[-\frac{5}{4}\left(\frac{f}{f_{peak}}\right)^{-4}\right] \gamma^b \quad (3.2)$$

where

$$a_{JS} = 0.076 \left(\frac{U_N}{f_{peak} g}\right)^{0.22}, \quad b = \exp\left[-\frac{1}{2}\left(\frac{f/f_{peak} - 1}{\sigma}\right)^2\right].$$

The values of the energy scale parameter a_{JS} , the peak enhancement factor γ , and peak width parameter σ are called the shape parameters. As these parameters change, the sea state spectrum changes. When $f \leq f_{peak}$, then σ is equal to the left peak width denoted by σ_1 . When $f > f_{peak}$, then σ is identical to the right peak width denoted by σ_2 . Furthermore, U_N is the wind speed measured by anemometer installed on weather ships at the height of N m above the sea surface. Since the JS model has a sharper peak than the PM spectrum, a peak-enhancement function γ^b is added to enhance its peak.

In addition, it is observed that the JS spectrum model has shown to be universally applicable for idealized fetch-limited conditions and also arbitrary wind conditions in deep water, including storms and hurricanes [17]. This experimental model is known to be more realistic than the PM spectrum model.

Sea surface moves all the time and thus renders link quality unstable. The sea wave movement continuously changes both maritime transceiver orientation and height, thus changing the maritime transceiver gain and received signal power.

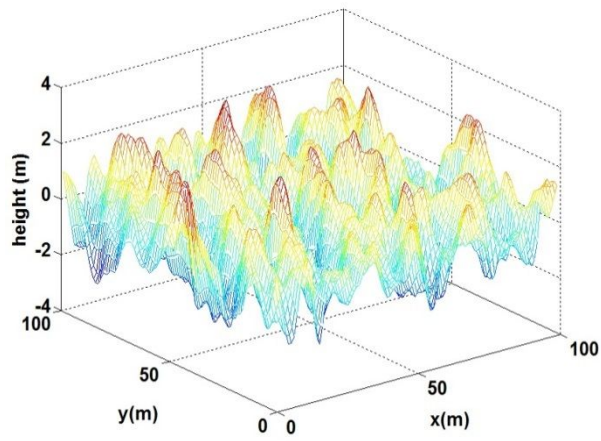
Since the real-time data is not available for our study, we have employed sea state data generated from the PM and JS spectrum models described

earlier. Table 3.1 shows the sea state parameters [19, 20]. The sea state conditions mentioned in Table 3.1 are a result of reflective nature of sea surface and wave height, which are measures of roughness of the sea parameters. Figure 3.1 shows the exemplary sea surface of the sea state 5 for PM and JS spectra.

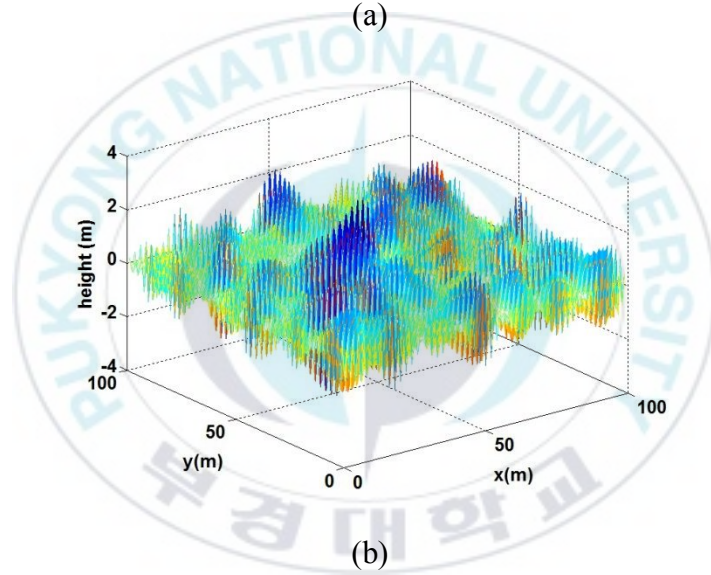
Table 3.1. Sea state parameters.

Sea state	Wind speed (m/s)	Average Wave period (sec)	Significant wave height (m)
4	8.33	4.6	1.2
5	11.11	6.2	2.5
6	13.89	7.7	4.5
7	16.67	10	7.1
8	22.23	12.4	14.3

At lower sea states, i.e. state 0 to 3, the sea conditions are mild, and hence the signal distortion is negligible at the receiver. While at higher states, sea conditions are hostile with relatively high waves and rapid moving winds. These would result in scattering of incoming signals, thus causing the signals to be extremely impaired at the receiver [21].



(a)



(b)

Figure 3.1. Sea surface from the spectra under sea state 5: (a) PM, (b) JS.

3.2. Atmospheric Turbulence

The atmospheric turbulence degrades the performance of a VLC link, because it causes fluctuation in both the amplitude and the phase of the received signal which vary randomly according to signal fading. Therefore, the wireless optical channel acts like a fading channel and its behavior can be modeled accurately using the appropriate statistical distribution on the atmospheric turbulence conditions.

The fading strength depends on the link length, the wavelength of the optical radiation and the refractive index structure parameter, C_n^2 , of the channel. The turbulence channel model is mathematically tractable and it is characterized by the log irradiance variance σ_I^2 . The log irradiance variance σ_I^2 can be calculated as [22]

$$\sigma_I^2 = 1.23 C_n^2 K^{7/6} L^{11/6} . \quad (3.3)$$

where K is the wave number ($2\pi/\lambda$), L is the distance between the transmitter and receiver of the optical wireless channel.

3.2.1. Log-Normal Turbulence Model

Atmospheric turbulence is usually categorized into regimes depending on the magnitude of the index of refraction variation and inhomogeneity. The

log-normal distribution is generally used to model the fading associated with the weak atmospheric turbulence regime [23]. In the following analysis, the weak turbulence is assumed and thus the log-normal atmospheric model is used for the evaluation. The probability density function of log-normal distribution of the received irradiance, I , is given by [23]

$$P(I) = \frac{1}{\sqrt{2\pi\sigma_i^2}} \frac{1}{I} \exp\left\{-\frac{(\ln(I/I_o) + \sigma_i^2/2)^2}{2\sigma_i^2}\right\} \quad I \geq 0. \quad (3.4)$$

It is characterized by the log irradiance variance σ_i^2 , a mean value of $\sigma_i^2/2$, and signal irradiance without scintillation I_o .

3.2.2. Gamma-Gamma Turbulence Model

For weak to strong turbulence conditions, a suitable statistical distribution for modeling the irradiance fluctuations is Gamma-Gamma [24]. The probability density function (PDF) of the Gamma-Gamma distribution as a function of I , is given by [24]

$$P(I) = \frac{2(\alpha\beta)^{(\alpha+\beta)/2}}{\Gamma(\alpha)\Gamma(\beta)} I^{\left(\frac{\alpha+\beta}{2}\right)-1} K_{\alpha-\beta}(2\sqrt{\alpha\beta I}) \quad I > 0. \quad (3.5)$$

where $K_n(\cdot)$ is the modified Bessel function of the second kind of order n , and $\Gamma(\cdot)$ represents the gamma function. If the optical radiation is assumed to

be a plane wave, the two parameters α and β that characterize the irradiance fluctuation PDF are related to the atmospheric conditions by

$$\alpha = \left[\exp\left(\frac{0.49\sigma_I^2}{(1+1.11\sigma_I^{12/5})^{7/6}}\right) \right]^{-1}, \beta = \left[\exp\left(\frac{0.51\sigma_I^2}{(1+0.69\sigma_I^{12/5})^{5/6}}\right) \right]^{-1}. \quad (3.6)$$

Table 3.2 gives the normal gamma-gamma turbulence parameters in turbulence conditions [25].

Table 3.2. Weak to strong turbulence regimes.

Parameter	Turbulence regime		
	weak	moderate	strong
σ_I^2	0.2	1.6	3.5
α	11.6	4.0	4.2
β	10.1	1.9	1.4

4. MVLC System Design

Figure 4.1 shows the proposed system in which communication coverage area can be increased at a very low-cost of implementation. The network is formed by neighboring ships, marine beacons and buoys. Maritime transceivers are located to connect to the terrestrial networks via VLC link. Lighthouses are assumed to operate as base stations. The lighthouse consists of power LEDs that provide coverage to a very large area, while maritime transceivers consist of an LED array and photodetectors (PDs).

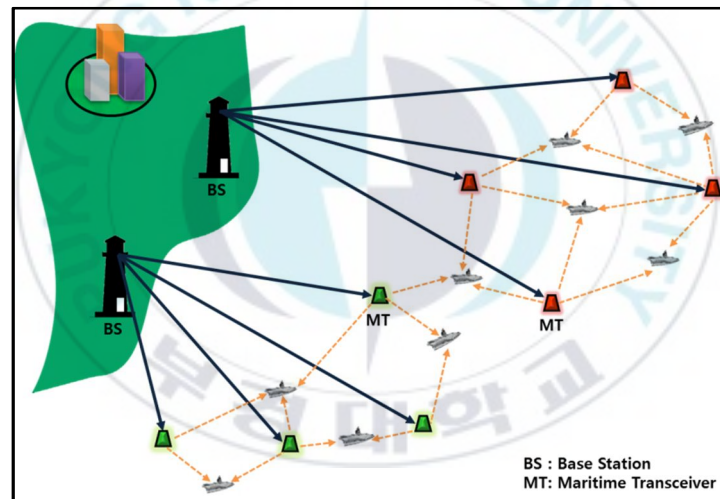


Figure 4.1. MVLC network

4.1. MVLC Channel Model

The study considers a maritime channel model where sea surface moves all the time and thus renders unstable link quality. The sea wave movement continuously changes both maritime transceiver orientation and height, thus changing the maritime transceiver gain and received signal power. Figure 4.2 shows the maritime channel model under sea states and atmospheric turbulence. It consists of the lighthouse and maritime transceivers placed over the sea.

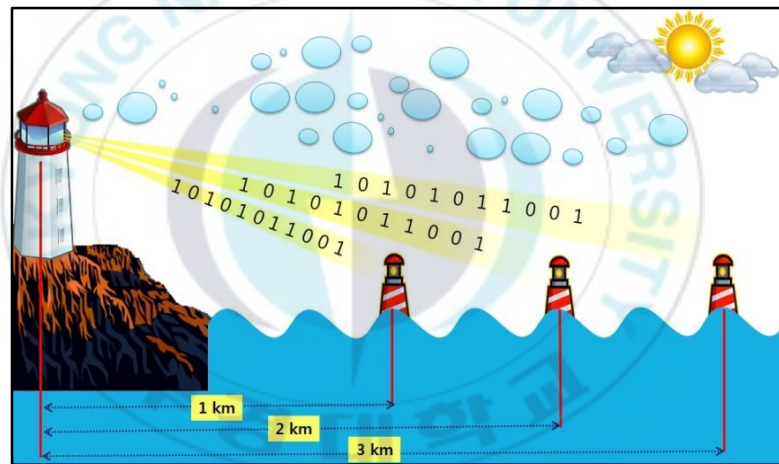


Figure 4.2. Maritime channel modeling.

Simulations were conducted to investigate the link performance for the proposed shore-to-sea MVLC link. It is worth noting that the transmitted optical power from relay was considered in accordance with the values

defined in International Association of Lighthouse Authorities (IALA)'s manual [26].

Table 4.1. Simulation parameters of the MVLC system

	Parameter	Value
Source	Transmitted optical power (All LEDs) in lighthouse	400 W
	Number of LEDs in lighthouse	100
	LED half angle	60°
	Luminous intensity (All LEDs)	12732 cd
	Type of PD	Si PIN
	Height of the lighthouse	50 m
	Height of the light source in lighthouse	48 m
Receiver	Detector physical area (each PD)	3 x 3 cm ²
	Receiving plane dimension	10 m x 10 m
	Field of view	50°
	Refractive index of a lens at receiver	1.2
MVLC	Sea state	[4, 5, 6, 7, 8]
Channel	Sea spectrum model	Pierson-Moskowitz, JONSWAP
	Atmospheric turbulence model	Log-Normal, Gamma-Gamma

4.2. MVLC Receiver

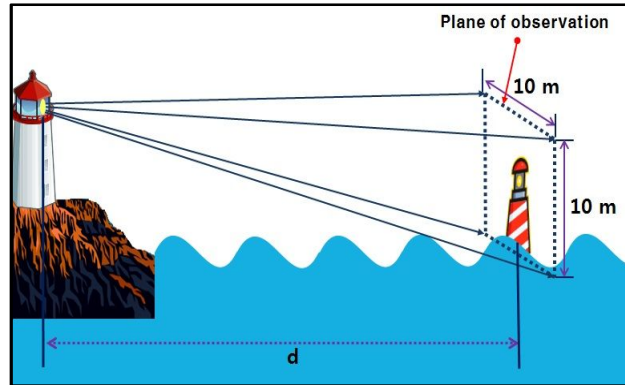


Figure 4.3. Receiving plane ($10\text{ m} \times 10\text{ m}$)

The receiving plane is assumed to be $10\text{ m} \times 10\text{ m}$ over a maritime transceiver as shown in Figure 4.3.

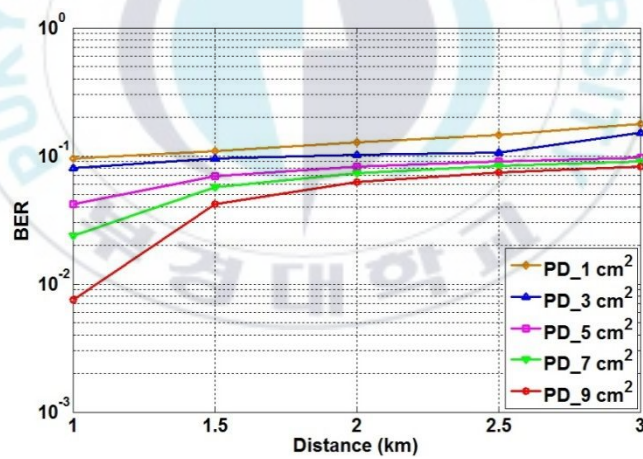


Figure 4.4. BER performance comparison relative to PD physical area.

The simulation performed for various apertures of PDs under sea state 5 with log-normal turbulence based on the JS model. Observing the results from

Figure 4.4, it can be said that with the increasing aperture of the PD, the effect of atmospheric turbulence can be reduced.



5. Performance Analysis of the MVLC System

As described in Chapter 1, the target of this study is to develop a high-performance MVLC system with the fulfilled objectives given. In order to materialize the objectives, several simulations were performed on the MVLC system described in Chapters 3 and 4.

5.1. Shore-to-Sea Transmission in MVLC

Shore-to-sea maritime communication using visible light transmission is proposed. As it is based on LEDs for data transmission, it offers a low-cost, high-speed and low power consumption communication system for maritime users. The proposed transmission scheme considers unique properties of maritime environments where wave height, wind speed, etc. exist. Computer simulations are conducted based on the PM and JS spectrum models with various sea states for analysis.

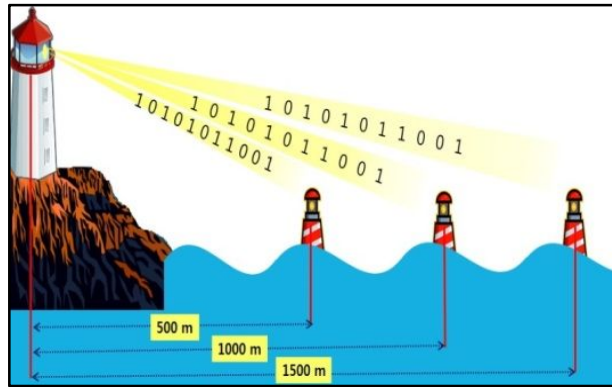
5.1.1. Shore-to-Sea Visible Light Transmission

Since the real-time data is not available for the present study, we employ sea state data from PM spectrum model and JS spectrum model for performing simulations as it was developed from real measurements of

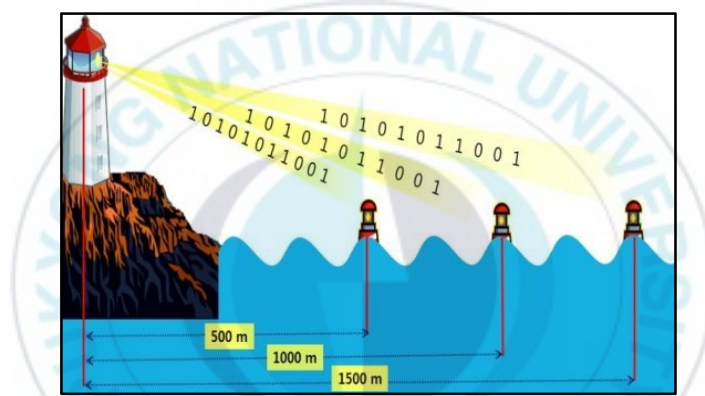
various sea parameters. This model is based on new theory of sea behavior assuming that if the wind blew for a long time over a large sea area, the waves would come into equilibrium with the wind. This is the concept of a fully developed sea.

The sea waves are often portrayed as having a normal sine wave nature, however, by actual experiments they are described as a Trochoid [27]. At lower sea states, i.e. state 0 to 3, the sea conditions are mild, and hence the signal distortion is negligible at the receiver. While at higher states, sea conditions are hostile with relatively high waves and rapid moving winds. These would result in scattering of incoming signals, thus causing the signals to be extremely damaged at receiver [21].

Sea surface moves all the time and thus renders link quality unstable. The sea wave movement continuously changes the maritime transceiver orientation and height, thus changing the maritime transceiver gain and received signal power. Figure 5.1 shows the present maritime channel model under consideration. It consists of lighthouse and maritime transceivers placed over the sea.



(a)



(b)

Figure 5.1. Shore-to-sea channel model: (a) Sea state 4, (b) Sea state 8.

5.1.2. Performance Analysis

Simulation has been carried out to investigate the link performance for the proposed shore-to-sea MVLC system. Performance is evaluated in terms

of bit error rate (BER) against signal-to-noise ratio (SNR) values with respect to distance between lighthouse and maritime transceivers. We obtained the BERs for the proposed MVLC system by using the sea state data from PM and JS spectrum. In line of sight (LOS) channel, the light from transmitter is directed towards the receiver where we measured SNRs and BERs.

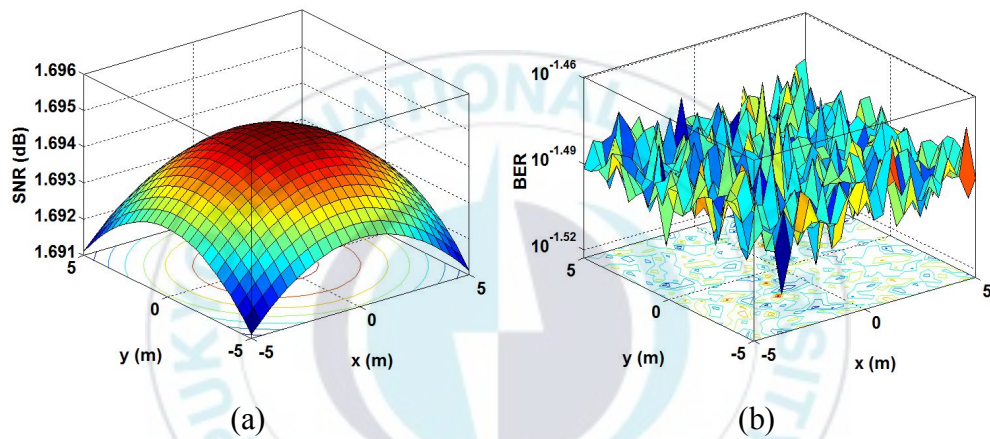


Figure 5.2. Simulated proposed channel with PM spectrum: (a) SNR, (b) BER.

Figure 5.2 shows the performance of the proposed channel model for PM spectrum under sea state 5, where transmitter and receiver are separated over a distance of 1 km. Figure 5.3 shows the performance of the channel between the transmitter and the receiver at the distance of 1 km apart with sea state 5 of JS spectrum.

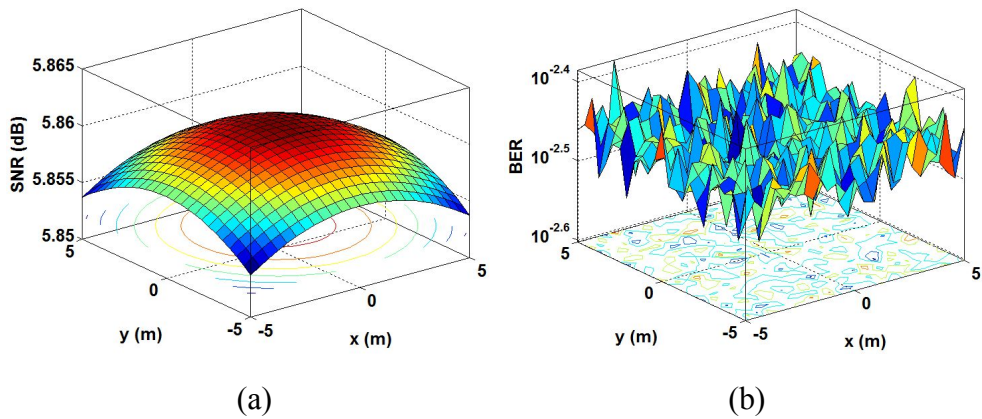


Figure 5.3. Simulated proposed channel with JS spectrum: (a) SNR, (b) BER.

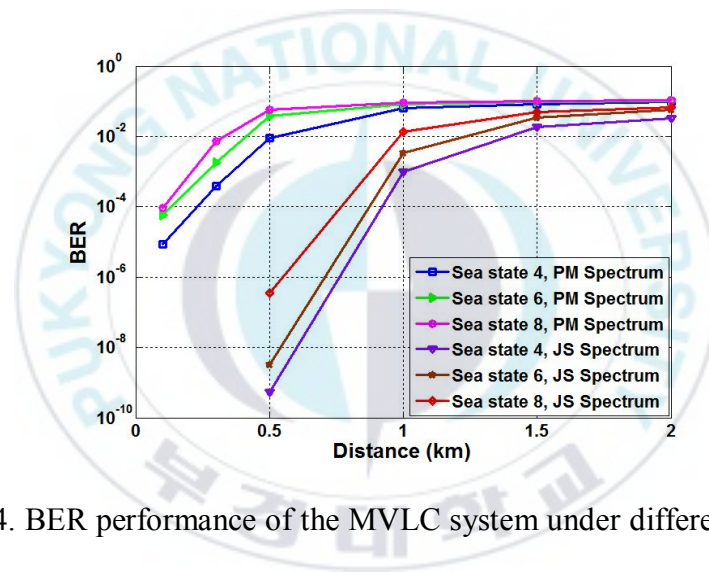


Figure 5.4. BER performance of the MVLC system under different sea states.

Figure 5.4 shows the analysis of the MVLC system under the sea state 4, 6 and 8. Overall, the JS model outperforms the PM in terms of BER. The JS model for sea state 6 shows a performance of 10^{-3} at the distance of approximately 1 km. However, the BER performances at a larger distance

between the transmitter and the receiver are poor, thus requiring higher LED power.

5.2. Shore-to-Sea MVLC using Color Clustered MIMO

Shore-to-sea visible light communication using color clustered MIMO is presented in this section. The proposed MVLC offers a low-cost, high-speed wireless link for shore-to-sea maritime communications. Each color cluster is comprised of 50 red, green and blue (RGB) LEDs and is modulated using on-off-keying (OOK). Selection combining (SC) is performed at the receiver, producing diversity effect within that color cluster. In this paper, we employ sea states data from both PM and JS spectrum models under log-normal turbulence conditions. Based on the simulation model, the maritime link quality is analyzed in terms of coverage distance and BER performance.

5.2.1. Color Clustered MIMO VLC

Figure 5.5 오류! 참조 원본을 찾을 수 없습니다.(a) portrays the MVLC system under consideration. The lighthouse shown in Figure 5.5 오류! 참조 원본을 찾을 수 없습니다.(a) consists of a power LED array that provides coverage to a very large area. The maritime transceivers are composed of an

LED array for transmission and photodetectors and filters for reception. A VLC link is established between the lighthouse and the maritime transceiver, considering sea state and log-normal turbulence.

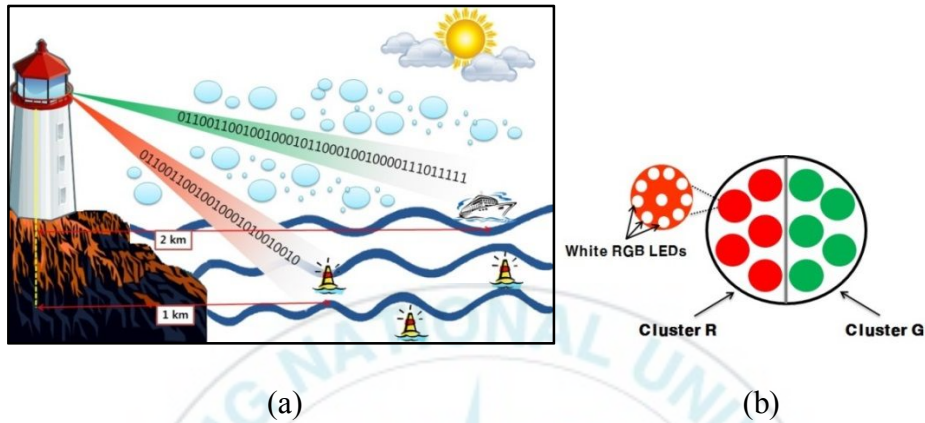


Figure 5.5. Color-clustered MVLC system (a) Conceptual design, (b) RG LED array.

The maritime system comprises various marks such as lighthouses, maritime transceivers, laser markers etc., which act as visual aids for ships and boats. Providing illumination and direction to ships are another aid of lighthouse and maritime transceivers. For this purpose, we designed a power LED array that consists of two color clusters, i.e. red and green, of LEDs as shown in Figure 5.5 오류! 참조 원본을 찾을 수 없습니다.(b). Each color cluster consists of 50 RGB LEDs where data bits for communication are modulated and transmitted using individual color from LEDs. The red and

green colors used in the proposed scheme for color clustered MIMO are in line with the maritime buoyage system defined by IALA.

Figure 5.6 shows the block diagram of the transmitter used in the proposed system. Input binary sequence is divided into two parallel streams, one for each color cluster. The data stream is modulated in each cluster by using the OOK modulation scheme, where each LED in a cluster transmits the same data stream. At the receiver in Figure 5.6, the three photodetectors in each color cluster are installed in addition to the color filter. The received signal from each photodetector is compared with the signals received from the other photodetectors (i.e. SC) [28]. Thus, the color clustered MIMO method increases diversity gain and contributes to a significant improvement in the performance of the proposed MVLC system.

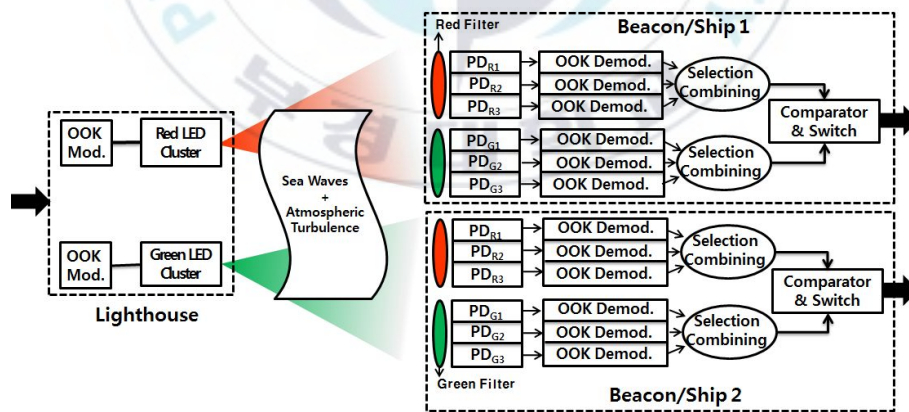


Figure 5.6. Block diagram of the proposed system.

5.2.2. Performance Analysis

Simulations have been carried out to analyze the link performance of the proposed shore-to-sea MVLC using color clustered MIMO. Performance is evaluated in terms of BER with respect to distance between lighthouse and receivers. Figure 5.7(a) shows the analysis of a conventional MVLC system under various sea states and log-normal turbulence using the OOK modulation technique. It can be observed from the simulation results that the JS spectrum model with sea state 4 only appears appropriate for communication up to approximately 1 km using the underlying LED and photo detector combination, whereas the performance severely degrades in PM spectrum model. It is also observed that at higher sea states the transmission channel condition becomes hostile from high wind speed, wave height, etc., resulting in degraded performance as shown in Figure 5.7(a).

Figure 5.7(b) shows the analysis of the MVLC link using the color clustered MIMO. It is apparent that the BER performance of the proposed scheme is significantly improved compared with the conventional MVLC based simple OOK transmission. In particular, the JS spectrum model offers a BER of 10^{-3} at a distance of 1.5 km for sea state 4. At this performance criterion, the conventional VLC achieves a distance of 1 km. Therefore, the

proposed color clustered MIMO scheme can increase the distance of transmission in MVLC environments without increasing the transmission power. As the distance increases, it is obvious that the BER performances degrade. This degradation can be compensated using powerful error detection and correction coding.

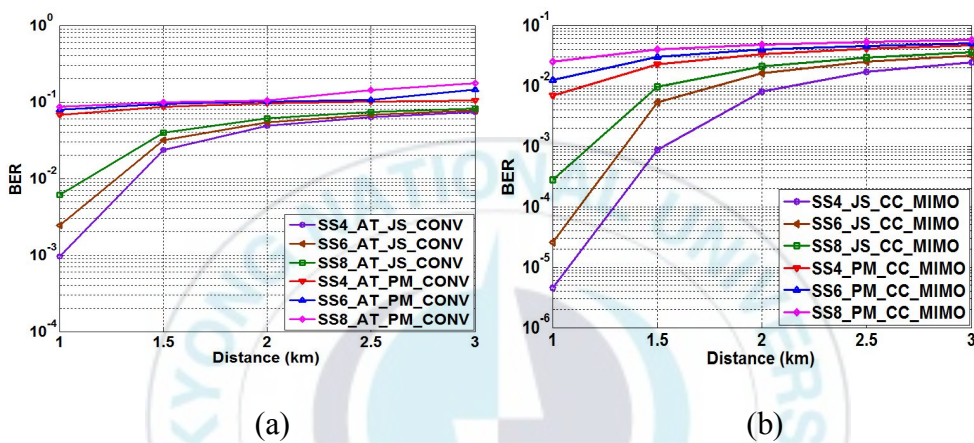


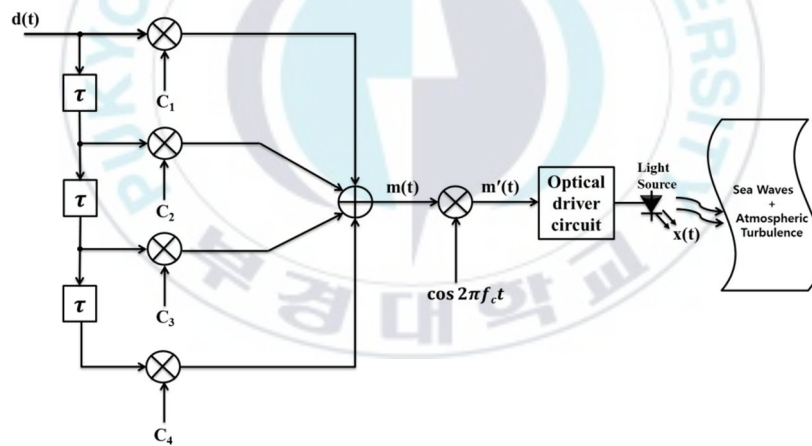
Figure 5.7. Performance analysis of MVLC link: (a) Conventional VLC, (b) Color Clustered MIMO based MVLC.

5.3. Time-Code Diversity (TCD) Scheme for MVLC

This chapter presents a novel TCD based shore-to-sea maritime data transmission system using visible light in maritime environments to overcome the limitations of conventional maritime wireless communications.

We first analyzed the MVLC on the basis of unique properties of a maritime environment, i.e. sea states and atmospheric turbulence using JS spectrum models. In order to combat maritime fading conditions that significantly degrade the performance and coverage distance, we propose a TCD scheme in which the delayed versions of the original data are retransmitted using orthogonal Walsh codes. This TCD scheme is found to be superior in that it offers three orders of magnitude in terms of BER performance, compared with non-TCD conventional transmission scheme.

5.3.1. TCD Scheme for MVLC



(a)

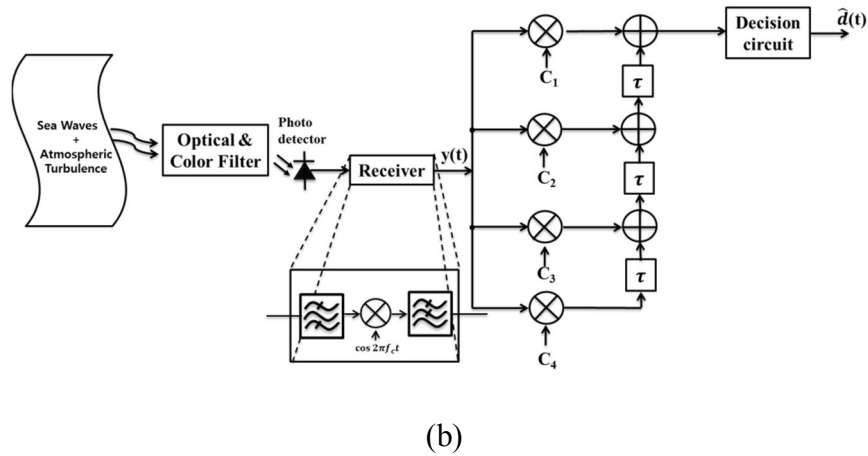


Figure 5.8. Block diagram of the TCD scheme: (a) Transmitter, (b) Receiver.

In order to improve the performance of the MVLC over various sea states, we propose a TCD, in which the original signal and its 3 delayed versions are transmitted by employing orthogonal Walsh codes of length 4. The value of delay, τ , can be decided on the basis of maximum coverage distance, d . In this case, the value of τ is calculated to be $10 \mu\text{s}$, i.e. $\tau = d / c$, where $d = 3 \text{ km}$ and $c = 3 \times 10^8 \text{ m/s}$. In other words, the delay of 1 bit is assured since the bit duration and the value of τ is identical, i.e. $10 \mu\text{s}$. This transmission strategy would yield diversity gain through the reception of multiple transmitted signals. The block diagram of the transmitter for the proposed TCD based VLC system is shown in 오류! 참조 원본을 찾을 수

없습니다.(a). The data and its three delayed versions are spread using orthogonal codes. After spreading, the composite signal is formed by adding all the signals from the direct path and its delayed versions. This composite signal is transmitted by LEDs after multiplying with the frequency f_c . Then, the signal propagates through the channel and suffers from various sea states and atmospheric turbulence conditions as noted earlier. The transmitted signal is given by

$$m'(t) = \sum_{i=1}^4 d(t-(i-1)\tau) c_i \cos 2\pi f_c t. \quad (5.1)$$

where $d(\cdot) \in [0,1]$ and τ represents the path delay shown in 오류! 참조 원본을 찾을 수 없습니다.(a). c_i represents code sequence separated by the code for $i \in [1,2,3,4]$.

At the receiver, an optical filter is installed prior to the PD for reducing the effect of ambient light noise and sunlight [29]. The block diagram of the receiver is shown in 오류! 참조 원본을 찾을 수 없습니다.(b). The received signal is then passed through coherent demodulator to recover the low pass signal. The filtered signal from the demodulator is then fed to receive the original data by multiplying with respective orthogonal codes. The decision

circuit will then estimate the data. In this way, the demodulated and estimated data is compared with originally transmitted to produce the BER.

At the receiver side, the received signal can be modeled as [30]

$$y(t) = RI[1 + \zeta m(t)] + n(t). \quad (5.2)$$

R denotes the PD's responsivity, I is the received optical irradiance, ζ is the modulation index and $n(t)$ is the additive white Gaussian noise (AWGN) whose variance is σ^2 and this variance is computed from $\sigma^2 = (\sigma_B)^2 + (\sigma_T)^2$. σ_B^2 is the background noise composed of a shot noise because of the radiation from sky and sun, and σ_T^2 is the total thermal noise at the receiver.

The sum of the demodulator outputs is then fed into the decision circuit as shown in 오류! 참조 원본을 찾을 수 없습니다.(b). At this point, the electrical SNR can be described as

$$SNR = \frac{P_m}{\sigma^2}. \quad (5.3)$$

The average received optical power, P_m , is given by

$$P_m = \frac{A^2}{2T} \int_0^T g^2(t) dt. \quad (5.4)$$

where A is the symbol amplitude and T is the symbol duration. $g(t)$ is the pulse shaping function that is included in the optical driver unit.

5.3.2. Performance Analysis

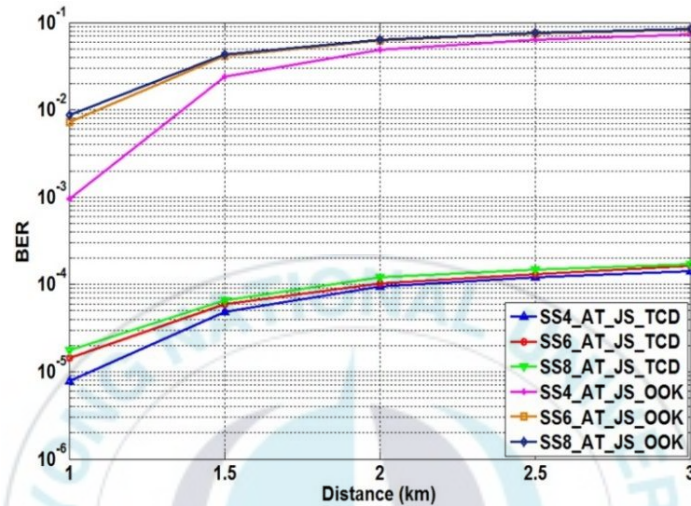


Figure 5.9. BER performance comparison of OOK and TCD MVLC systems with the sea states and log-normal turbulence from JS model.

We performed a comparative study between a representative transmission scheme of VLC, i.e. conventional OOK and the proposed TCD scheme. We also used the previously defined MVLC channel i.e. the JS spectrum model under log-normal turbulence conditions. The results of this comparative analysis are shown in Figure 5.9. It is remarkable that the proposed scheme based on TCD produces approximately a BER performance of 10^{-5} at a

distance of 1 km. Even when the distance is increased, it still outperforms the conventional OOK scheme. Overall, it is found that the TCD offers three orders of magnitude in terms of BER performance, compared with the OOK transmission scheme. Therefore, the proposed TCD can be regarded as an excellent performance-enhancing scheme applicable to the MVLC transmission scenarios.

5.4. MVLC Links Employing Multi-hop Relay

This chapter presents a multi-hop relay VLC system for maritime applications. MVLC systems suffer from limited coverage distance due inherently to the usage of LEDs and PDs. The proposed system employs a multiple decode-and-forward (DF) relays to extend coverage distance in maritime environments. The multi-hop relay based MVLC is analyzed under a maritime channel modeled by the JS spectrum and gamma-gamma distribution. It is found that the use of relays in maritime environments can extend the coverage distance significantly and also improve the performance. In addition, the performance of the system is analyzed using various combining techniques at the receiver to enhance the performance. The

maximal ratio combining (MRC) technique is found to provide superior link quality under maritime environments.

5.4.1. Multi-hop Relay based MVLC

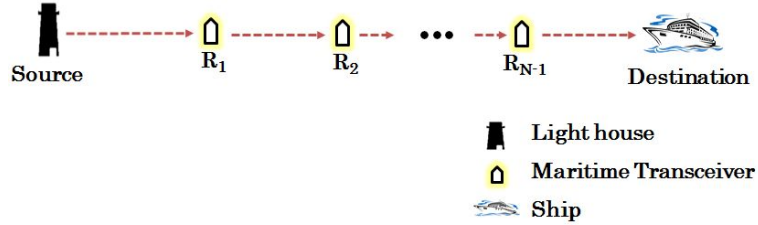


Figure 5.10. Multi-hop relay MVLC system.

A MVLC multi-hop (maritime transceiver) communication system using DF relays is shown in Figure 5.10. The intensity modulation/direct detection (IM/DD) link using OOK is considered. The source is a lighthouse that communicates with the destination terminal through R_i , $i = 1, 2, \dots, N-1$, optical maritime transceivers. These act as relay nodes, all being in equidistance. Assuming that there are k hops and $(N-1)$ DF relays between the source and the destination, r_k is the received signal at hop k and is given by

$$r_k = x\eta I_k + n_k, \quad k = 1, \dots, N. \quad (5.5)$$

where $x \in \{0, 1\}$ represents the information bits, η is the optical-to-electrical conversion coefficient. Note that hop k is referred to as the link between $(k-1)^{th}$ relay and k^{th} relay. For $k = 1$, I_k denotes the irradiance from the transmitter (lighthouse) and for $k = 2$ through N , I_k represents the irradiance from the $(k-1)^{th}$ relay at the k^{th} receiver, and n_k is AWGN with zero mean and variance of $N_o/2$. It can be assumed that the presence of ambient light in PDs can be ignored under the Gaussian noise approximation [31]. Furthermore, although the ambient light is a major source of interference particularly during the daytime, it can be significantly reduced using optical filters over the PDs in practical VLC implementations [31, 29].

The equivalent end-to-end SNR, i.e. the SNR (μ) at the receiver, can be written as [32]

$$\mu = \left(\sum_{k=1}^N \frac{1}{\mu_k} \right)^{-1}. \quad (5.6)$$

where $\mu_k = (\eta I_k)^2 / N_o$ is the instantaneous SNR at the k^{th} hop.

Assuming that all hops have the same statistical behavior, an approximated BER can be calculated by [33]

$$BER \approx \frac{1}{2} (1 - (1 - 2BER_k)^N).$$

(5.7)

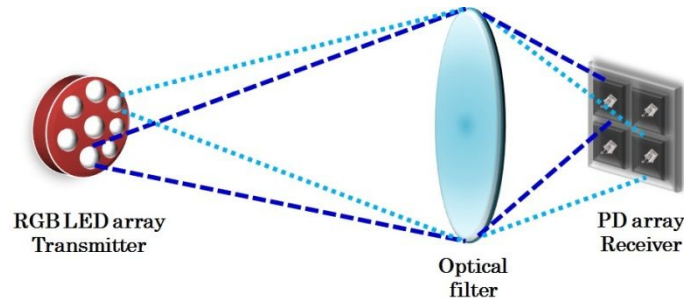


Figure 5.11. PD array-based VLC.

One of the possible methods of reducing atmospheric turbulence is the use of aperture averaging [34]. In the aperture averaging, the receiver aperture needs to be far greater than the spatial coherence distance of the atmospheric turbulence in order to receive several uncorrelated signals. This condition is only achieved in FSO when the aperture size is on the order of centimeters since the spatial coherence distance is on the order of centimeters [35]. Hence, we utilized a PD array whose area is $3 \times 3 \text{ cm}^2$ (2×2 PDs, each with an area of $1.5 \times 1.5 \text{ cm}^2$) and performed receiver diversity techniques. In order to exploit diversity gain over an array of PDs, three combining schemes were employed in the present work and compared in terms of performance: SC, equal gain combining (EGC) and MRC [36].

To derive a closed-form analysis, we first develop a statistical model for the combined electrical SNR at the receiver. Among the considered combining schemes, the SC is the simplest since it processes only one of the diversity apertures or specifically the aperture with the maximum received irradiance (or electrical SNR). Therefore, the selection is made according to

$$I_{sc} = \max(I_1, I_2, \dots, I_4). \quad (5.8)$$

The received signal and average SNR at the output of SC receiver can be expressed as

$$r_{sc} = \frac{x\eta}{4} I_{sc} + n_k, \quad k = 1, \dots, N \quad (5.9)$$

$$\mu_{sc} = \frac{(\eta I_{sc})^2}{4N_o}. \quad (5.10)$$

For the case where EGC is implemented at the receiver, the received signal and SNR can be expressed as

$$r_{EGC} = \frac{x\eta}{4} \sum_{m=1}^4 I_{k,m} + n_k, \quad k = 1, \dots, N. \quad (5.11)$$

$$\mu_{EGC} = \frac{\eta^2}{16N_o} \left(\sum_{m=1}^4 I_{k,m} \right)^2, \quad k = 1, \dots, N. \quad (5.12)$$

In the case of MRC, the combined signal and SNR are given as

$$r_{MRC} = \frac{x\eta}{2} \sqrt{\sum_{m=1}^4 I_{k,m}^2 + n_k}, \quad k = 1, \dots, N. \quad (5.13)$$

$$\mu_{MRC} = \frac{\eta^2}{4N_o} \sum_{m=1}^4 I_{k,m}^2, \quad k = 1, \dots, N \quad (5.14)$$

5.4.2. Performance Analysis

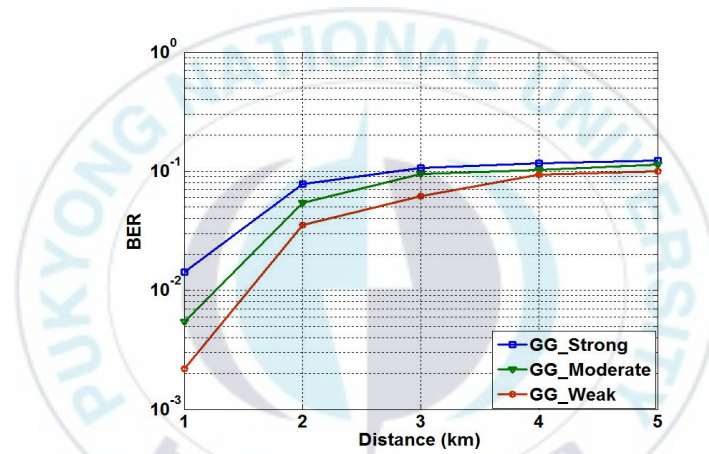


Figure 5.12. Comparison of BER performance over each gamma-gamma turbulence strength

Figure 5.12 shows the comparison of BER performances over each gamma-gamma turbulence condition at a larger distance between the transmitter and the receiver. It is found that the BER of the system increases

with the increase of the value of Rytov variance (from weak to strong turbulence). It is also observed that the BER performances at a larger distance between the transmitter and the receiver are poor. Therefore, a few compensation techniques are required, such as partially coherent beam, aperture averaging, adaptive optics and spatial diversity [34].

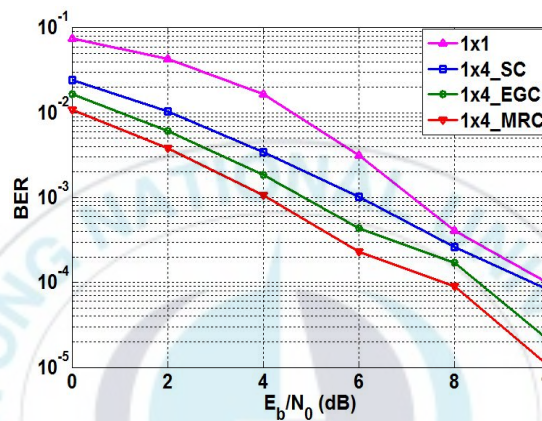


Figure 5.13. BER performance relative to the received power level

Furthermore, we performed a comparative study with the PD array based diversity combining techniques. Figure 5.13 depicts the BER performance comparison among the combining techniques over the sea state 4 and the weak turbulence condition. At a SNR value of 10 dB, the average BERs of the diversity combining techniques are better than 10^{-4} , while the BER of the non-diversity scheme is just 10^{-4} . Note that for a fair comparison, an identical

PD area of $3 \times 3 \text{ cm}^2$ for all PDs was considered for the diversity schemes. By the same token, the PD area for the non-diversity scheme (1×1 in Figure 5.13 and

Figure 5.14) is also ensured to be $3 \times 3 \text{ cm}^2$, although it appears to be impractical.

Finally,

Figure 5.14 shows the BER performance relative to the number of hops between the transmitter and the receiver with the combining techniques. The distance between the transmitter and the receiver is set to 5 km. It is clear that there is an increasing gap in terms of BER over the considered combining techniques as the number of hops increases. However, it is found that the proposed multi-hop relay based maritime system with the MRC technique provides the best link quality under the maritime environments; it achieves a BER of approximately 10^{-5} with 4 relays for the transmission.

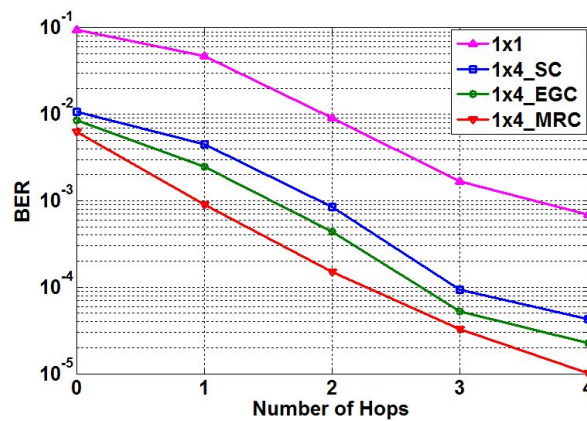


Figure 5.14. BER performance relative to the number of hops with diversity combining techniques

5.5. MVLC in Fog Conditions

Performances of a MVLC link and visibility range are adversely affected by weather conditions like fog, rain, clouds snowfall etc. and atmospheric turbulence like scintillation. With the motivation for providing an efficient VLC link under sea states affected by fog conditions, a realistic analysis of MVLC is presented using JS spectrum model with sea state parameters applied, along with Kim's model for fog attenuation characteristics. This section presents a simulation based model in which the maritime link quality is analyzed in terms of coverage distance and BER performance.

5.5.1. Analysis Fog Conditions for MVLC

For clear or foggy weather Kim's model based on the visibility range estimate is employed to compute the attenuation. Mostly used value of the transmittance threshold level (T_{th}) is 2% along the propagation path. The attenuation for Kim model is given by [37]

$$\alpha = \frac{\ln(T_{th})}{V} \left(\frac{\lambda}{550} \right)^{-q} = \frac{3.912}{V} \left(\frac{\lambda}{550} \right)^{-q} \quad [\text{dB/km}] . \quad (5.15)$$

where V stands for visibility, λ in nm stands for wavelength, q is the size distribution of the fog droplets and rely on various visibility range values. Figure 5.15 shows different color wavelength attenuation under fog condition.

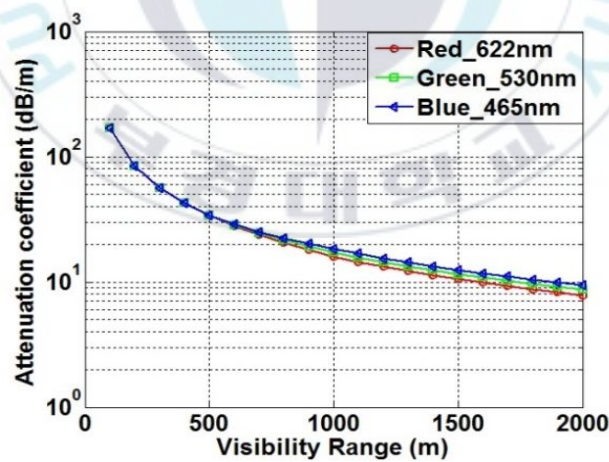


Figure 5.15. Kim model for visibility for T_{th} of 2% and a range of RGB LED.

5.5.2. Performance Analysis

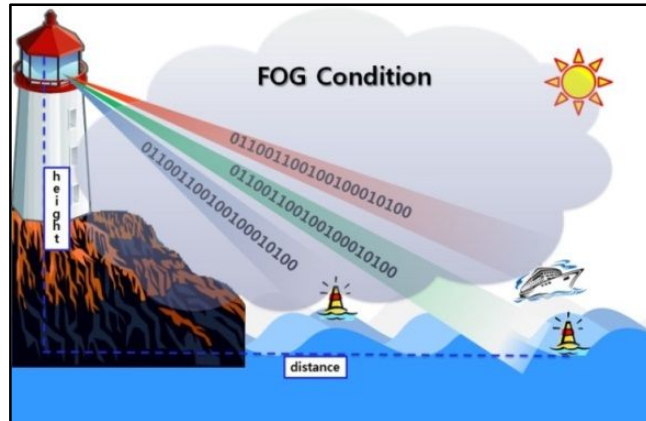


Figure 5.16. Shore-to sea transmission channel modeling: Sea state and fog condition.

We performed simulations in a MVLC environment having the proposed LED setup as shown in Figure 5.16. The reception is performed at various distances, i.e. at 200 m to 1,000 m.

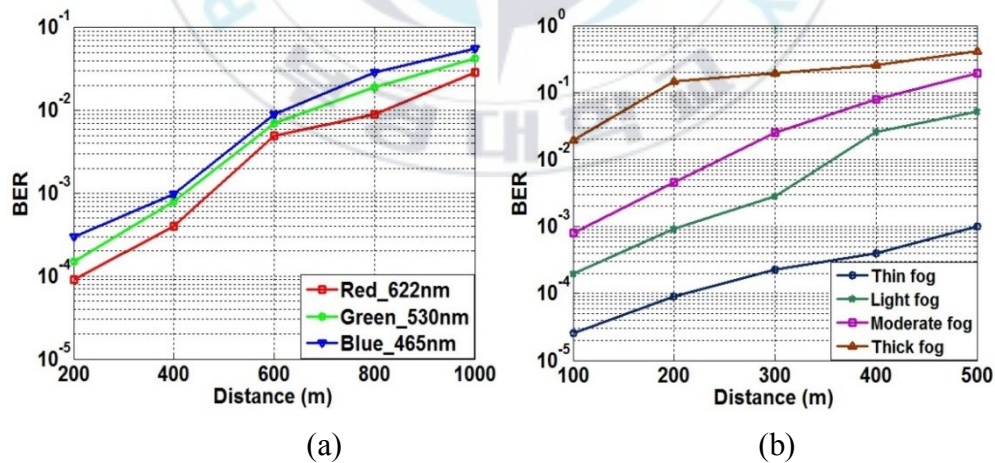


Figure 5.17. Comparative analysis of BER performance for MVLC link:

(a) Utilizing various color wavelengths in thin fog, (b) Under various fog conditions using red color wavelength.

Figure 5.17(a) shows the comparative analysis of MVLC link using RGB LED when the sea state is 5 and fog condition is thin fog condition (visibility range: 1900~2000 m). It is apparent from Figure 5.17(a) that the BER performance of the red color wavelength is better than other color wavelengths. Additionally, the simulations are also performed to obtain BER performance with respect to increasing distance under various fog conditions using red color wavelength, when the sea state of maritime environment is sea state 5. Figure 5.17(b) shows the BER comparison under various fog conditions.

6. Conclusions

In this thesis, we presented the performance of the MVLC system in various maritime environments. The MVLC system encompasses visible light transmission using LEDs and photodetectors for the transmission between shore and sea. The heavy reliance on RF communication networks would create bandwidth insufficiency for high-resolution sensors and equipment and also would be unable to provide capability for jamming. Therefore, the MVLC can be an attractive candidate for advanced maritime broadband communications.

In the first study, VLC system is proposed for maritime environments and analyzed relative to distance, based on JS and PM sea spectra. Performance evaluation has been conducted using the PM and JS models. The performance relative to the sea states varies in terms of distance. It is shown that the JS model appears to be more realistic and produce better performance over a larger distance.

Secondly, the MVLC system with the color clustered MIMO is proposed and analyzed relative to distance based on PM and JS sea spectrum models under log-normal turbulence. The proposed system encompasses VLC using LEDs and photodetectors for the transmission between shore and sea. The

performances relative to the sea states and atmospheric turbulence vary in terms of distance. It is found that at high sea states, a more rigorous transmission scheme needs to be employed. Recognizing the limitations of the existing maritime communication networks such as a lack of bandwidth and the installation of expensive network infrastructure, the proposed color clustered MIMO based MVLC can be an attractive candidate for an advanced maritime broadband communication system. The results show that the proposed system provides an efficient MVLC, while satisfying IALA requirements for maritime buoyage system and also offering sufficient illumination from high power LEDs.

In the third study, a MVLC system with the TCD scheme has been proposed and analyzed based on the JS sea spectra under log-normal turbulence. This TCD scheme is found to be superior in that it offers three orders of magnitude in terms of BER performance, compared with non-TCD conventional transmission scheme. The proposed scheme is robust and efficient to overcome the effect of impairments present in maritime environments with a BER of approximately 10^{-5} and a data rate of 100 Kbps at a distance of 1 km.

In the fourth study, a generalized multi-hop VLC system over maritime channels with DF relays is presented. The performance of the proposed multi-hop MVLC system was analyzed considering various noise parameters in maritime environments, such as sea states and gamma-gamma turbulence. Furthermore, in order to enhance the performance, the diversity combining techniques were utilized. It is found that the MRC scheme gives a superior BER performance at a 5 km distance with 4 relays installed at equidistance.

In the final study, a system is proposed for maritime environments and analyzed relative to visibility distance, based on JS sea spectra under various fog conditions. For clear or foggy weather Kim's model is employed to compute the attenuation. The proposed system encompasses visible light transmission using LEDs and photodetectors for the transmission between shore and sea, considering signal attenuation due to various fog conditions. It can be concluded that, under various fog conditions, red color wavelength gives better performance than any other color wavelength. Hence, usage of red color for transmission in a maritime environment is most favorable. As future work, the present study with fog conditions can further be extended for heavy rain and atmospheric turbulence conditions to obtain the most desirable VLC link in maritime environments.

References

- [1] T. Komine and M. Nakagawa, "Fundamental analysis for visible-light communication system using LED lights," *IEEE Transactions on Consumer Electronics*, vol. 50, no. 1, pp. 100-107, 2004.
- [2] S. Rajagopal, R. D. Roberts and S. K. Lim, "IEEE 802.15.7 visible light communication: modulation schemes and dimming support," *IEEE Communications Magazine*, vol. 50, no. 3, pp. 72-82, 2012.
- [3] C. X. Wang, F. Haider, X. Gao, X. H. You, Y. Yang, D. Yuan, H. Aggoune, H. Haas, S. Fletcher and E. Hepsaydir, "Cellular architecture and key technologies for 5G wireless communication networks," *IEEE Communications Magazine*, vol. 52, no. 2, pp. 122-130, 2014.
- [4] T. Yokotani, "Application and technical issues on Internet of Things," in *The 10th International Conference on Optical Internet (COIN)*, Yokohama, Japan, 2012.
- [5] S. Arnon, "Optimised optical wireless car-to-traffic-light communication," *Transactions on Emerging Telecommunications Technologies*, vol. 25, no. 6, pp. 660-665, 2014.

- [6] D. Dhatchayeny, A. Sewaiwar, S. Tiwari and Y. H. Chung, "Experimental Biomedical EEG Signal Transmission using VLC," *IEEE Sensors Journal*, vol. 15, no. 10, pp. 5386-5387, 2015.
- [7] IMO and COMSAR, "Harmonization of GMDSS Requirements for Radio," 2004.
- [8] "IMO website," [Online]. Available:
http://www.imo.org/blast/mainframe.asp?topic_id=69&doc_id=581#dsc.
- [9] IALA, "The IALA definition and vision for e-Navigation," 2007.
- [10] M. Zhou, V. D. Hoang, H. Harada, J. S. Pathmasuntharam, H. Wang, P. Y. Kong, C. W. Ang, Y. Ge and S. Wen, "TRITON: high-speed maritime wireless mesh network," *IEEE Wireless Communications*, vol. 20, no. 5, pp. 134-142, 2013.
- [11] "ESA telecommunication & integrated applications website," [Online]. Available: telecom.esa.int/telecom/www/object/index.cfm?fobjectid=9121.
- [12] C. F. Lin, "An advance wireless multimedia communication application: mobile telemedicine," *WSEAS Transactions on Communications*, no. 9, pp. 203-215, 2010.

- [13] A. Asosheh, A. Afshinfar, M. Kharrat and N. Ramezani, "A network model for the intelligent marine container tracking," in *8th WSEAS International Conference on Applied Informatics and Communications (AIC)*, Rhodes, Greece, 2008.
- [14] G. Cossu, R. Corsini, A. M. Khalid, S. Balestrino, A. Coppelli, A. Caiti and E. Ciaramella, "Experimental demonstration of high speed underwater visible light communications," in *2nd International Workshop on Optical Wireless Communications (IWOW)*,, 2013.
- [15] VLCC, "Lighthouse sub project," 2007. [Online].
Available: <http://www.vlcc.net>.
- [16] M.-T. Zhou and H. Harada, "Cognitive maritime wireless mesh/ad hoc networks," *Journal of Network and Computer Applications*, vol. 35, no. 2, pp. 518-526, 2012.
- [17] L. H. Holthuijsen, *Waves in Oceanic and Coastal Waters*, Cambridge University Press, 2007.
- [18] D. E. M. D. a. J. A. E. Hasselmann, "Directional wave spectra observed during JONSWAP 1973," *Journal of physical oceanography*, vol. 10, no. 8, pp. 1264-1280, 1980.

- [19] R. P. Pinet, Invitation to Oceanography, Jones & Bartlett Learning, 2015.
- [20] "National Marine Weather Guide," Government of Canada and Environment Canada, [Online]. Available: <http://ec.gc.ca/meteor-weather/default.asp?lang=En&n=279AC7ED-1&offset=3&toc=show>.
- [21] K. Ward, C. Baker and S. Watts, "Maritime surveillance radar. I. Radar scattering from the ocean surface," *Radar and Signal Processing, IEE Proceedings F*, vol. 137, no. 2, pp. 51-62, 1990.
- [22] X. Zhu and J. Kahn, "Free-space optical communication through atmospheric turbulence channels," *IEEE Transactions on Communications*, vol. 50, no. 8, pp. 1293-1300, 2002.
- [23] R. L. Phillips and L. C. Andrews, "Universal statistical model for irradiance fluctuations in a turbulent medium," *Journal of Optical Society of America*, vol. 72, no. 7, pp. 864-870, 1982.
- [24] M. Uysal, J. Li and M. Yu, "Error rate performance analysis of coded free-space optical links over gamma-gamma atmospheric turbulence channels," *IEEE Transactions on Wireless Communications*, vol. 5, no. 6, pp. 1229-1233, 2006.

- [25] X. Zhu and J. Kahn, "Performance bounds for coded free-space optical communications through atmospheric turbulence channels," *IEEE Transactions on Communications*, vol. 51, no. 8, pp. 1233-1239, 2003.
- [26] "Aids to Navigation Manual," International Association of Lighthouse Authorities, [Online]. Available: <http://www.puertos.es/Documents/7-NAVGUIDE%202014%20not%20printable.pdf>.
- [27] S. Wen, P. Y. Kong, J. Shankar, H. Wang, Y. Ge and C. W. Ang, "A Novel Framework to Simulate Maritime Wireless Communication Networks," in *IEEE OCEANS 2007*, 2007.
- [28] P. P. Han, A. Sewaiwar, S. V. Tiwari and Y. H. Chung, "Color-clustered multiple-input multiple-output visible light communication," *Journal of the Optical Society of Korea*, vol. 19, pp. 74-79, 2015.
- [29] Y. H. Kim and Y. H. Chung, "Experimental Outdoor Visible Light Data Communication System using Differential Decision Threshold with Optical and Color Filters," *Optical Engineering*, vol. 54, p. 040501, 2015.
- [30] W. O. Popoola, Z. Ghassemlooy, J. I. H. Allen, E. Leitgeb and S. Gao, "Free-space optical communication employing subcarrier modulation and spatial diversity in atmospheric turbulence channel," *IET*

optoelectronics, vol. 2, no. 1, pp. 16-23, 2008.

- [31] T. Tsiftsis, H. Sandalidis, G. Karagiannidis and M. Uysal, "Optical wireless links with spatial diversity over strong atmospheric turbulence channels," *IEEE Transactions on Wireless Communications*, vol. 8, no. 2, pp. 951-957, 2009.
- [32] M. Hasna and M. S. Alouini, "Outage probability of multihop transmission over Nakagami fading channels," *IEEE Communications Letters*, vol. 7, no. 5, pp. 216-218, 2003.
- [33] E. Morgado, J. I. Mora, J. Vinagre, J. Ramos and A. Caamano, "End-to-End Average BER in Multihop Wireless Networks over Fading Channels," *IEEE Transactions on Wireless Communications*, vol. 9, no. 8, pp. 2478-2487, 2010.
- [34] X. Zhu and J. Kahn, "Performance bounds for coded free-space optical communications through atmospheric turbulence channels," *IEEE Transactions on in Communications*, vol. 51, no. 8, pp. 1233-1239, 2003.
- [35] X. Zhu and J. Kahn, "Free-space optical communication through atmospheric turbulence channels," *IEEE Transactions on Communications*, vol. 50, no. 8, pp. 1293-1300, 2002.

- [36] M. K. Simon and M. S. Alouini, Digital communication over fading channels, John Wiley & Sons, 2005.
- [37] I. Kim, B. McArthur and E. Korevaar, "Comparison of Laser Beam Propagation at 785 and 1550 nm in Fog and Haze for Optical Wireless Communications," *Proc. SPIE*, vol. 4214, pp. 26-37, 2001.



List of Publications

Journal Papers:

- [1] **Hyeongji Kim**, Atul Sewaiwar and Yeon-Ho Chung, "High-Performance Time-Code Diversity Scheme for Shore-to-Sea Maritime Visible-Light Communication," *Journal of the Optical Society of Korea*, Vol. 19, Issue 5, pp. 514-520 (2015). (SCIE, I.F. 1.17)
- [2] **Hyeongji Kim**, and Yeon-Ho Chung, "Shore-to-sea Maritime Visible Light Communication using color Clustered MIMO," *Journal of the Korean Institute of Information and Communication Engineering*, Vol. 19, Issue 8, pp. 1773-1779 (2015). (KCI)
- [3] **Hyeongji Kim**, Atul Sewaiwar, and Yeon-Ho Chung, "Maritime Visible Light Communication with Sea Spectrum Models," *International Journal of Communications*, Vol. 9, pp. 67–70 (2015). (EI)
- [4] **Hyeong-Ji Kim**, Samrat Vikramaditya Tiwari, and Yeon-Ho Chung, "Multi-hop relay based maritime visible light communication," *Chinese Optics Letters*. (SCIE, I.F. 1.851) - Under review.

Conference Papers:

- [1] **Hyeongji Kim**, Atul Sewaiwar, and Yeon-Ho Chung, "Shore-to-Sea Maritime Communication with Visible Light Transmission" *in* The 2014 International Conference on Communications and Computers, Saint Petersburg, State Politechnical University, Russia, September 23-25, 2014.
- [2] **Hyeong-Ji Kim**, Samrat V. Tiwari, Phyu Phyu Han, and Yeon-Ho Chung, "Performance Evaluation of Maritime LED Broadband Communication Systems using Maritime Wireless Channel" *in* The 2014 Conference on Electronics and Communication, Changwon, Changwon University, South Korea, Jun 7, 2014.
- [3] Phyu Phyu Han, Atul Sewaiwar, **Hyeong-Ji Kim**, and Yeon-Ho Chung, "Performance Evaluation of MIMO Visible Light Communication System" *in* The Korean Institute of Information, Electronic and Communication Technology (KIIECT), vo. 7, no. 1, pp. 75-78, South Korea, May 16-17, 2014.

감사의 글

먼저 석사 과정 동안 연구에 매진할 수 있도록 아낌없는 격려와 지도를 해주신 정연호 교수님께 진심으로 감사드립니다. 그리고 저의 논문 심사를 맡아주시고, 소중한 충고와 조언을 해주셨던 정신일 교수님, 류지열 교수님께 깊은 감사를 드립니다.

2 년이라는 시간을 가족같이 함께한 이동전송시스템 연구실 선후배에게도 깊은 감사의 인사를 드립니다. 연구실의 제일 큰 언니로 후배들을 챙겨주시는 Phyu Phyu Han, 성실한 연구 자세를 몸소 보여준 동기 Atul, Samrat, 그 외 많은 이동전송시스템 연구실 대학원생과 학부생들에게도 그 동안의 즐거운 추억들이 영원하길 바랍니다. 그리고 석사 졸업생 민지, 준영이에게도 앞날이 늘 화창하기를 기원합니다.

저의 넋두리를 들어주며 격려하고 응원해준 친구 가란, 나리, 보람, 성희에게도 항상 고맙고, 지금의 모습 변하지 않고 영원히 친하게 지내길 바랍니다. 그리고 힘들고 괴로운 일이 있을 때마다 즐거움을 준 동원이, 정신적으로 후원해줬던 태우, 재은이에게 고맙습니다.

항상 응원해 주신 할아버지, 늘 제 곁에서 믿어주시고 뒷바라지 해주신 사랑하는 부모님, 격려를 아끼지 않았던 병주, 이제는 이러한 가족들의 기대에 부응하고 은혜에 조금이나마 보답할 수 있도록 노력할 것이라고 전하고 싶습니다.

마지막으로 지면으로 통해서 일일이 언급을 하지 못했지만 그동안 저를 아끼고 사랑해주신 모든 분들께 다시 한 번 진심으로 감사드립니다.



2016년 1월

김형지 올림